Stability of steady flow through an axially corrugated pipe

S. A. Loh and H. M. Blackburn
Department of Mechanical and Aerospace Engineering, Monash University, Clayton, VIC 3800, Australia

(Received 14 July 2011; accepted 20 October 2011; published online 17 November 2011)

The linear stability of steady flow in pipes with circular cross-section and sinusoidal axial variation in diameter is studied by finding global eigenmodes with axial wavelength commensurate with that of the wall corrugation, chosen to be equal to one pipe mean radius. The maximum peak-to-peak height of corrugation considered is approximately 8% of the mean diameter. At low corrugation amplitude and at low Reynolds numbers, the base flow remains attached to the wall, while at larger amplitudes and Reynolds numbers, an axisymmetric separation bubble forms within the corrugation. For all Reynolds numbers considered, flows remain stable to axisymmetric perturbations, but become unstable to standing-wave modes of low azimuthal wavenumber, with critical Reynolds number first falling, then increasing with increasing corrugation height. Both attached and separated flows exhibit similar types of instability modes, which in the case of separated flow are most energetic near the reattachment line of the base flow. The leading instability modes consist of counter-rotating vortices situated near the pipe wall. © *2011 American Institute of Physics*. [doi:10.1063/1.3660522]

The stability of fully developed flow in straight-walled pipes of circular section has been extensively studied and it is generally accepted[1–3] that the flow is linearly stable to infinitesimal perturbations, gives rise to moderate linear transient energy growth whose magnitude scales with the square of Reynolds number,[4] supports equilibrium (but unstable) travelling-wave states of finite amplitude, and becomes turbulent in practice at a range of bulk-flow Reynolds numbers $Re = U_{\text{bulk}}\ D/\nu = 4Q/(\pi D\nu)$ starting at approximately 2000. The size of flow perturbations which trigger transition falls with Reynolds number, again for Reynolds numbers larger than approximately 2000.[5] The travelling waves are associated with longitudinal rolls and axial streaks and it has recently been suggested that the equilibrium states can be obtained as solutions of a nonlinear eigenproblem involving a coupling of these basic flow elements.[6]

All real pipes have some degree of geometric imperfection, which may be randomly distributed (e.g., "commercial roughness"), or more organized, either by manufacture (e.g., machining or deliberately introduced during forming for the case of flexible segmented pipelines and ducts) or from scale deposition in process equipment. It is notable that over a large range of surface roughness, typically observed transition Reynolds numbers remain in the range 2000–3000,[7,8] suggesting that the basic mechanism of instability remains the same in the presence of wall roughness.

Compared to the situation for flow perturbation in straight pipes, the effect of wall shape variation on pipe flow stability has received little systematic attention. Arguably, the simplest case for study is presented by a sinusoidal axial variation in diameter where the corrugation amplitude is described by $\alpha = 0.5(D_{\max} - D_{\min})/D_{\text{mean.}}$ Experimental studies have mainly concentrated on comparatively large corrugation amplitudes $(\alpha \simeq 0.3 - 0.5)$ and on the enhancement of transfer processes by unsteadiness. At $\alpha = 0.3$ Deiber and Schowalter[9] observed the onset of turbulence at $Re \simeq 500$ while for $\alpha = 0.54$ Nishimura *et al.*[10] observed onset at $Re \simeq 200$. To our knowledge, there are only two pre-existing analyses of flow stability in corrugated pipes. Lahbabi and Chang[11] dealt with linear stability at one comparatively large wall corrugation amplitude, $\alpha = 0.3$. They concluded that for disturbances with the same axial periodicity as the corrugation, axisymmetric disturbances were stable at Reynolds numbers up to approximately 800 (the highest in their study), and non-axisymmetric instability arose via a Hopf bifurcation at $Re_c \approx 200$ in azimuthal wavenumber $k = 1$, leading to helical wave-like instabilities. The study of Cotrell *et al.*[12] was primarily concerned with instabilities in the low corrugation amplitude limit, considered disturbances whose axial wavenumbers were in general incommensurate with that of the corrugation and concentrated on axisymmetric disturbances with $k = 0$. Their analysis was carried out for corrugations of axial wavelength equal to the mean radius. According to their results, axisymmetric disturbances are the least stable at low corrugation amplitude, $\alpha < 0.1$, but for finite corrugation amplitude, critical axisymmetric disturbances were found at axial wavelengths shorter than, and incommensurate with, that of the corrugation. In the low-amplitude limit, the axial wavelength for critical instability tended to that of the corrugation. At larger corrugation amplitudes, non-axisymmetric disturbances were said to be less stable and eventually to dominate, although this part of their investigation was "cursory." We note that their study of non-axisymmetric disturbances was apparently confined to $k \leq 2$.

Various stability analyses of planar flows with corrugated walls have appeared. The most directly relevant of these is that of Floryan,[13] which dealt with linear stability of Poiseuille flow in a converging-diverging channel. In contrast to flows in a cylindrical geometry, plane Poiseuille flow is unstable to two-dimensional Tollmein–Schlichting waves in the $\alpha \to 0$ limit. Floryan showed that for quite small wave heights, of order $\alpha = 0.01$ in our measure, the flows are

however first linearly unstable to longitudinal-vortex-type standing wave modes commensurate with the corrugation wavelength. The underlying mechanism was attributed to centrifugal instability i.e., of Taylor–Görtler type.

Analogous to Floryan's study, the present work deals primarily with asymptotic instabilities in corrugated pipes whose global modes are assumed to have the same axial wavelength as the corrugation (since axial periodicity is imposed on both the base and perturbation flows) and considers (similar to Cotrell *et al.*) an axial wavelength to radius ratio of unity and corrugation amplitudes $\alpha < 0.08$. Our results show that, contrary to those earlier findings, the least stable cases at low-to-moderate corrugation amplitude occur with non-axisymmetric disturbances, albeit typically with $k = 3$ or 4. Critical Reynolds numbers are significantly lower than those found by Cotrell *et al*. Unstable modes take the form of radially compressed counter-rotating vortex pairs situated near the pipe wall, and, in cases where the flow separates, having greatest energy near the reattachment line of the base flow.

Choosing the mean pipe diameter $D_{\mathrm{mean}} = (D_{\mathrm{max}} - D_{\mathrm{min}})/2$ as the length scale, the non-dimensional radius of the pipe wall is given by $R(z) = 0.5[1 + \alpha \cos(2\pi z/\Lambda)]$ where z is the axial coordinate and Λ is the corrugation wavelength. As stated above, this study is confined to $\Lambda = 0.5$, and we have considered the five dimensionless corrugation amplitudes listed in Table I.

The stability analysis considers linear perturbations to the incompressible Navier–Stokes equations, following well-established methodologies detailed elsewhere.[14–16] The underlying discretization employs nodal spectral elements and a cylindrical coordinate formulation.[17] Base flows are obtained by direct numerical simulation of the axisymmetric Navier–Stokes equations in an axially periodic domain, with an axial body force replacing a mean axial pressure gradient, thus allowing the pressure to have axial periodicity. The base flows are time-marched to steady state and then supplied as data for the linear stability solver. Stability analysis is carried out using a timestepper-based method, using the same domain and mesh. Perturbation flows are taken to be zero at the walls and axially periodic. The action of the linear operator governing the evolution of perturbations is projected onto a low-dimensional Krylov subspace and an Arnoldi iteration method is used to extract dominant eigenvalues and modes. Separate analyses were carried out for each azimuthal wavenumber k.

All meshes used were composed of 16 spectral elements with shape functions in each element being tensor product Lagrange interpolants on a mapped Gauss–Lobatto–Legendre grid. Following a grid resolution study described below, 12th order Lagrange interpolants were used for all computations, resulting in 2405 collocation nodes in each mesh. A typical domain and mesh are shown in Fig. 1: corrugation is obtained by applying a cosine radial distortion to a rectangular mesh, and the example shows the mesh for the maximum corrugation amplitude employed.

Reynolds numbers are based on the volumetric flow rate Q of the base flow and mean pipe diameter; $Re = 4Q/(\pi D_{\mathrm{mean}}\ \nu)$. For each value of axial body force, Q was established through quadrature of the axial velocity profile, once the flow reached a steady state. We note that since the base flows are computed using the axisymmetric restriction of the unsteady incompressible Navier–Stokes equations, the fact that a steady state is reached demonstrates that the flow is stable to axisymmetric axially periodic perturbations (both standing and travelling) at the Reynolds numbers considered, however this was also confirmed through stability analysis.

Spatial convergence of the base flow and non-axisymmetric stability calculations were verified by a shape-function-order grid resolution study carried out for the largest corrugation amplitude and the highest Reynolds number considered. Grid resolution for the rest of the study was chosen such that at this most demanding extreme of the analysis envelope, further refinement produced changes in the steady state axial velocity less than 0.01%. At this level of refinement, the stability eigenvalues were converged to three significant figures or better. Stability analyses were carried out for azimuthal wavenumbers $0 \leq k \leq 6$.

Both attached and separated base flows were observed; examples are shown in Fig. 2. Flow separation occurs in the adverse pressure gradient region downstream of the maximum constriction, while reattachment occurs upstream of this location. For the range of Reynolds numbers examined, attached flow always occurred for the two lowest corrugation amplitudes, while separated flow always occurred for the remaining three amplitudes. As Reynolds number increased the separation and reattachment points moved upstream and downstream respectively, increasing the relative volume of the separation bubble.

TABLE I. Dimensionless corrugation amplitudes $\alpha = 0.5(D_{\mathrm{max}} - D_{\mathrm{min}})D_{\mathrm{mean}}$ considered in the present work.

α	0.0159	0.0318	0.0477	0.0636	0.0795

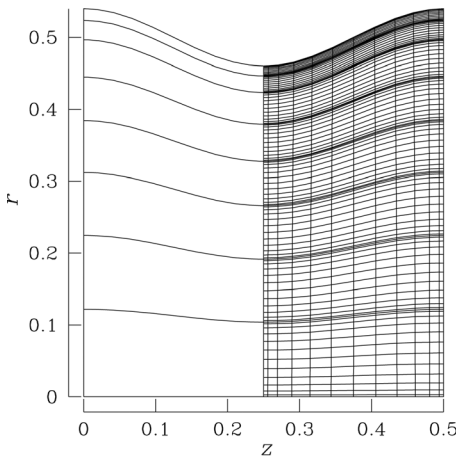

FIG. 1. Typical spectral element mesh in the meridional semi-plane, shown here for the maximum dimensionless corrugation amplitude considered, $\alpha = 0.0795$. Collocation nodes are shown for the resolution adopted in the study, with shape functions based on tensor products of 12th-order interpolants.

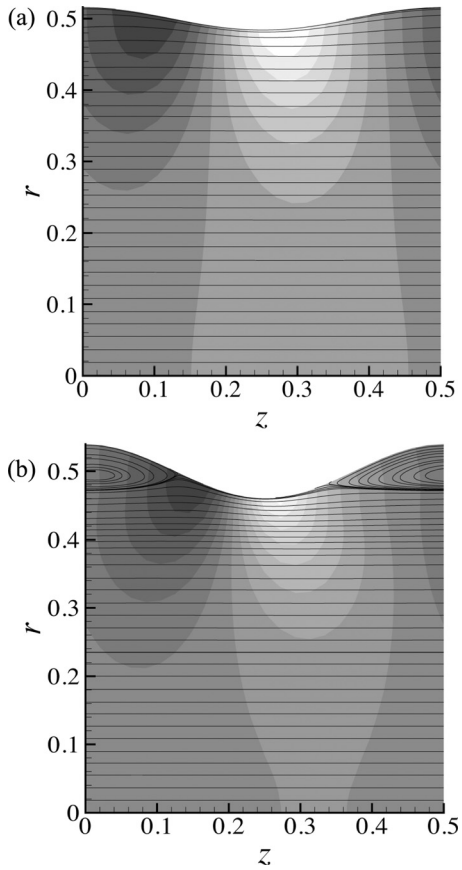

FIG. 2. Examples of attached and separated base flows, illustrated with streamlines and pressure contours (light/dark shading corresponds to low/high pressure). Bulk flow is from left to right. (a) attached flow, $Re = 2610$ and $\alpha = 0.0318$; (b) separated flow, $Re = 2200$ and $\alpha = 0.0795$.

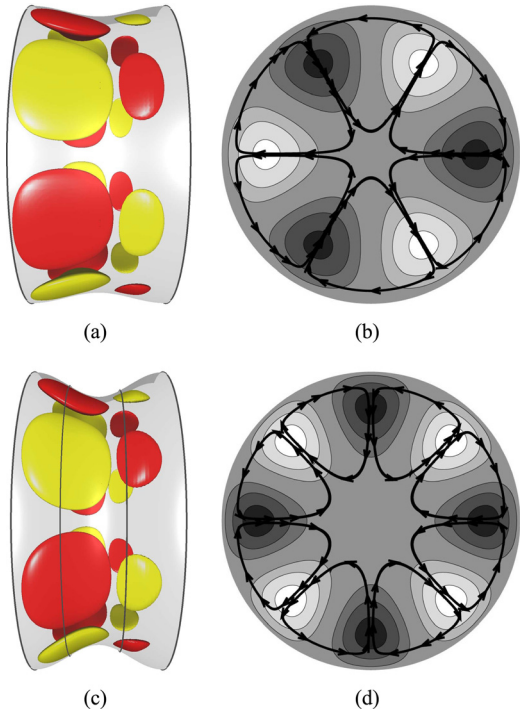

FIG. 3. (Color online) Typical unstable global modes visualized as (a) and (c) ± isosurfaces of azimuthal velocity component and (b) and (d) contours of axial velocity component (light/dark corresponding to positive/negative) at $z = 0.25$, with overlaid sectional streamlines. (a) and (b) attached flow, $Re = 3080$, $\alpha = 0.0318$, and $k = 3$; (c) and (d) separated flow (with reattachment/separation lines indicated in (c)), $Re = 2590$, $\alpha = 0.0795$, and $k = 4$.

Our analysis shows that for the corrugation amplitudes examined, these flows first become unstable to global modes with comparatively low azimuthal wavenumbers $k = 3$ and $k = 4$. Visualizations of representative leading global modes are shown in Fig. 3; the leading modes at different points in parameter space are quite similar in character to the examples shown. The isosurfaces of azimuthal velocity shown in Figs. 3(a) and 3(c) indicate that the critical modes take the form of arrays of counter-rotating longitudinal vortices which are stronger in the constricting sections of the pipe. We note however that the modes cannot be characterized as simple longitudinal vortices since the sense of rotation at any azimuthal location reverses on a traverse between the constricting and expanding sections of pipe. The sectional streamlines and axial velocity contours of Figs. 3(b) and 3(d) show the azimuthal symmetries of the modes at the axial station of maximum constriction and that, as could be expected, upwellings from the walls correspond to regions of negative axial perturbation velocity.

The presence of flow separation is not critical in determining the nature of the instability and it may be observed that the modes shown in Figs. 3(a) and 3(b) and Figs. 3(c) and 3(d), respectively, for attached and separated base flows, are qualitatively similar.

Fig. 4 shows the variation of critical Reynolds number with wall corrugation amplitude for non-axisymmetric disturbances as determined in the present study as well as the values reported by Cotrell *et al*. for axisymmetric disturbances.[12] In the range of corrugation amplitude examined, non-axisymmetric modes are the least stable.

As the corrugation amplitude becomes increasingly small, the critical Reynolds number becomes increasingly large, presumably asymptoting to infinity in the limit $\alpha \to 0$ as expected for stability of Hagen–Poiseuille flow. As the limit is approached, it may be that the critical modes are axisymmetric, and non-commensurate with corrugation wavelength, as reported by Cotrell *et al*. As the corrugation amplitude was increased the flow became increasingly unstable, with the minimum critical Reynolds number $Re_{c,\min} = 1971$ at $\alpha = 0.0636$, before increasing with further increases in the wall corrugation amplitude. At the lower corrugation amplitudes, the critical modes occur for $k = 3$, switching over to $k = 4$ at the largest amplitude considered, $\alpha = 0.0795$.

In order to check if axial subharmonic modes are less stable than those with the same axial periodicity as the corrugation, we carried out analysis at $\alpha = 0.0795$ on a domain with two corrugation modules. The least stable modes had the same eigenvalues as those for the single-module computations.

In comparing these results to corresponding analysis of planar corrugated channel flows,[13] we may note some strong similarities but also some differences. At equivalent corrugation amplitudes, the marginal stability Reynolds numbers predicted by Floryan are of the same order as, but significantly lower than, those in the present study.

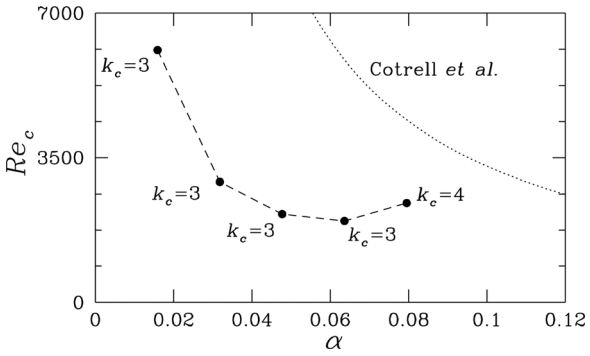

FIG. 4. Critical Reynolds numbers as functions of corrugation amplitude α for non-axisymmetric disturbances with critical azimuthal wave numbers labelled. Critical Reynolds numbers for axisymmetric disturbances reported by Cotrell *et al.*[12] are shown for comparison.

The leading instability mode shapes observed here (Fig. 3) show some similar features to those in the corrugated channel. While the dominant impression from sectional velocity fields is of arrays of longitudinal vortices that reach towards the location of largest axial velocity of the base flow, detailed study of flows near the corrugations reveals more structure, with the direction of swirl changing along a near-wall axial traverse. In the corrugated channel, the larger vortices reach across the centerline, but the near-wall structure is rather similar to what is observed here. An approximate conversion of the dominant cross-flow wavenumber found in that study corresponds to an azimuthal wavenumber $k=2$ in the present study, comparable to but smaller than the values $k=3$ and 4 that we have determined. It seems likely that the underlying instability mechanism is centrifugal in both studies.

In summary, our results suggest that wall corrugation, even of comparatively small amplitude, acts to destabilize laminar pipe flow. The most unstable modes are non-axisymmetric and in this study occurred for azimuthal wavenumbers $k=3$ and 4. One may expect that there is a relationship between the azimuthal wavenumbers of the critical modes and the axial wavenumber of the corrugation, such that a smaller corrugation wavelength could promote instability at larger azimuthal wavenumbers, a point we have not examined. Flow separation was not required for instability to arise.

We would like to acknowledge the contribution made in early stages of this work by T. Wallis.

[1]R. R. Kerswell, "Recent progress in understanding the transition to turbulence in a pipe," Nonlinearity **17**, R17 (2005).
[2]B. Eckhardt, T. M. Schneider, B. Hof, and J. Westerweel, "Turbulence transition in pipe flow," Annu. Rev. Fluid Mech. **39**, 447 (2007).
[3]T. Mullin, "Experimental studies of transition to turbulence in a pipe," Annu. Rev. Fluid Mech. **43**, 1 (2011).
[4]P. J. Schmid and D. S. Henningson, "Optimal energy density growth in Hagen–Poiseuille flow," J. Fluid Mech. **277**, 197 (1994).
[5]J. Piexinho and T. Mullin, "Finite amplitude thresholds for transition in pipe flow," J. Fluid Mech. **582**, 169 (2007).
[6]P. Hall and S. J. Sherwin, "Streamwise vortices in shear flows: Harbingers of transition and the skeletons of coherent structures," J. Fluid Mech. **661**, 178 (2010).
[7]J. Nikuradse, "Stromungsgesetze in rauhen Rohren," Forsch. Arb. Ing.-Wes. **361**, 1 (1933), reprinted as NACA TM-1292 (1950).
[8]G. Gioia and P. Chakraborty, "Turbulent friction in rough pipes and the energy spectrum of the phenomenological theory," Phys. Rev. Lett. **96**, 044502 (2006).
[9]J. A. Deiber and W. R. Schowalter, "Flow through tubes with sinusiodal axial variations in diameter," AIChE J. **25**, 638 (1979).
[10]T. Nishimura, Y. M. Bian, Y. Matsumoto, and K. Kunitsuga, "Fluid flow and mass transfer characteristics in a sinuoidal wavy-walled tube at moderate Reynolds numbers for steady flow," Heat Mass Trans. **39**, 239 (2003).
[11]A. Lahbabi and H.-C. Chang, "Flow in periodically constricted tubes: transition to inertial and nonsteady flows," Chem. Eng. Sci. **41**, 2487 (1986).
[12]D. L. Cotrell, G. B. MacFadden, and B. J. Alder, "Instability in pipe flow," Proc. Natl. Acad. Sci. **105**, 428 (2008).
[13]J. M. Floryan, "Vortex instability in a diverging-converging channel," J. Fluid Mech. **482**, 17 (2003).
[14]H. M. Blackburn, "Three-dimensional instability and state selection in an oscillatory axisymmetric swirling flow," Phys. Fluids **14**, 3983 (2002).
[15]S. J. Sherwin and H. M. Blackburn, "Three-dimensional instabilities and transition of steady and pulsatile flows in an axisymmetric stenotic tube," J. Fluid Mech. **533**, 297 (2005).
[16]D. Barkley, H. M. Blackburn, and S. J. Sherwin, "Direct optimal growth analysis for timesteppers," Int J. Numer. Methods Fluids **57**, 1437 (2008).
[17]H. M. Blackburn and S. J. Sherwin, "Formulation of a Galerkin spectral element–Fourier method for three-dimensional incompressible flows in cylindrical geometries," J. Comput. Phys. **197**, 759 (2004).